ISSN 1845–8319

OBSERVATIONS OF CHROMOSPHERIC EVAPORATION FLOWS IN RHESSI MICROFLARES

S. BERKEBILE-STOISER[1], P. GÖMÖRY[1,2], A. M. VERONIG[1]
and J. RYBÁK[2]

[1]*IGAM and Kanzelhöhe Observatory, Institute of Physics, University of Graz, Universitätsplatz 5, 8010 Graz, Austria*
[2]*Astronomical Institute, Slovak Academy of Sciences, SK-05960 Tatranská Lomnica, Slovakia*

Abstract. We present the analysis of two homologous microflares of GOES class <A9 with respect to mass flows in the chromosphere and transition region. Both events show non-thermal emission (evidence for beamed electrons) in RHESSI X-ray spectra. As outlined by observations of the Coronal Diagnostic Spectrometer, we find for the first event downflows in the He I, O V and Ne VI line reaching speeds up to 40 km s^{-1} at the position of chromospheric flare brightenings. On the other hand, upflows with velocities $\lesssim$40 km^{-1} are observed for the second microflare.
According to hydrodynamic flare simulations, the non-thermal electron energy density F deposited in the chromosphere determines if chromospheric evaporation is 'gentle' or 'explosive'. Thus, we derive rough estimates for F in our microflares and compare the results to the observed CDS flow properties.

Key words: flares - chromospheric evaporation - spectroscopy

1. Introduction

Hot plasma with temperatures $\gtrsim$ 10 MK observed in solar flares is thought to be generated in the process of 'chromospheric evaporation' (Neupert, 1968). Non-thermal electrons accelerated in the magnetic reconnection process in the corona are spiralling towards the transition region and chromosphere where they are stopped by Coulomb collisions. The energy lost by these non-thermal electrons causes strong heating of the chromospheric plasma which expands upwards into the coronal part of the flare loop, emitting in soft X-rays. Hydrodynamic simulations of electron driven chromospheric evaporation suggest that the response of the chromosphere to the heating process is dependent on the energy flux density of non-thermal electrons deposited in the chromosphere (Fisher *et al.*, 1985a,b,c). For low flux density, the evaporated plasma reaches speeds of several tens of km s^{-1} and the heated chromosphere is expanding, so called 'gentle' evaporation. For flares depositing large non-thermal energy flux density in the chromosphere, high velocities of several times the sound speed are expected for plasma flowing into the corona whereas the chromospheric material beneath is pushed down due to momentum conservation (Fisher, 1989), so called 'explosive' evaporation.

Evidence for flows in excess of $\sim$100 km s^{-1} was reported by, e.g. Doschek *et al.* (1980), Mariska *et al.* (1993) and Brosius and Phillips (2004) using SMM/BCS and Yohkoh/BCS data. Studies of flows in the EUV (observations of transition region plasma) with the Coronal Diagnostic Spectrometer implemented on the Solar and Heliospheric Observatory (CDS) which features excellent spatial resolution comprise Milligan *et al.* (2006), Brosius (2003), Teriaca *et al.* (2006) and Falchi *et al.* (2006). Several papers exist which report evaporation flows in medium and large flares. However, reports about flow dynamics in microflares are rare. Microflares are flares with a thermal energy content of 10^{-3} to 10^{-6} times the energy of very large flares (see e.g. Aschwanden, 2004) and are important in the frame of the micro- and nanoflare coronal heating model. The X-ray spectra of microflares evidence the existence of accelerated electrons (see e.g. Hannah *et al.*, 2008) and their multi-wavelength characteristics are in basic agreement with the ones expected for reconnection driven flares (e.g. Stoiser *et al.*, 2007). It can thus be supposed that non-thermal electrons can drive chromospheric evaporation in microflares and that we should be able to observe the associated flows. One of the rare spectroscopic observations of microflares using Hinode/EIS (Extreme Ultraviolet Imaging Spectrometer) is given in Milligan (2008) who reported direct heating of coronal plasma instead of evaporation in a small C class flare.

We here present observations of two microflares of GOES class <A9 which were observed at high spectral and spatial resolution by CDS and in RHESSI X-rays. We derive the velocity evolution in chromospheric and transition region lines and compare the observed flow characteristics to the predictions of hydrodynamic simulations.

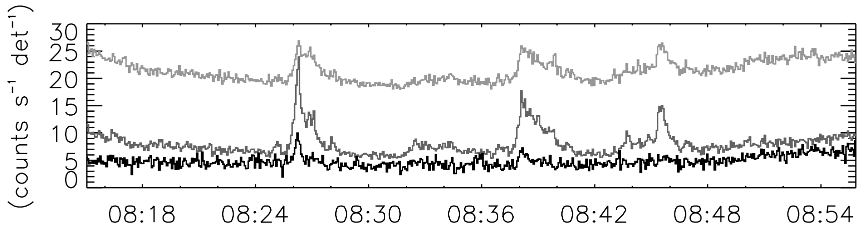

Figure 1: RHESSI X-ray light curves for the period July 4, 2006, 08:15 UT – 09:00 UT in the energy bands 3–6 keV (light grey), 6–9 keV (dark grey) and 9–15 keV (black). The microflares under study peaked at ∼08:26:20 UT and ∼08:38:10 UT.

2. Data

We present results of a data set acquired on July 4, 2006 during a joint observing campaign (JOP 171) for which SOHO/CDS, the Michelson Doppler Imager (SOHO/MDI), the Transition Region and Coronal Explorer (TRACE) and the Dutch Open Telescope (DOT) were coordinated. CDS observed among others emission lines of the following ions: He I (58.43 nm, $T \sim 3.9 \times 10^4$ K), O V (62.97 nm, $T \sim 2.6 \times 10^5$ K) and Ne VI (56.28 nm, $T \sim 4.2 \times 10^5$ K). The CDS slit ($2'' \times 240''$, pixel size $2'' \times 1.6''$) was set fixed in a sit-and-stare mode pointing to $X = 106''$ East and $Y = -149''$ South of the disc centre. CDS acquired observations at a cadence of 15 s. The line profiles were fitted with a broadened Gaussian profile. MDI provided high resolution magnetograms (pixel size of $\sim 0.6''$) and TRACE observed in the 17.1 nm passband (pixel size of $0.5''$, temporal resolution ∼90 s). The CDS and TRACE data were reduced by standard solar software routines. For microflare identification as well as X-ray spectroscopy we used observations of the Reuven Ramaty High Energy Solar Spectroscopic Imager (RHESSI) which observes flare X-ray emission $\gtrsim$3 keV for the full Sun. Data recorded by the CDS, TRACE and MDI were co-aligned by 2-dimensional cross-correlation of images recorded at similar temperatures.

3. Event Overview

On July 4, the instruments of the observing campaign were pointed to AR 10898 (Mt. Wilson class β) consisting of a sunspot embedded in enhanced magnetic flux of the opposite polarity. On this day, we found 2

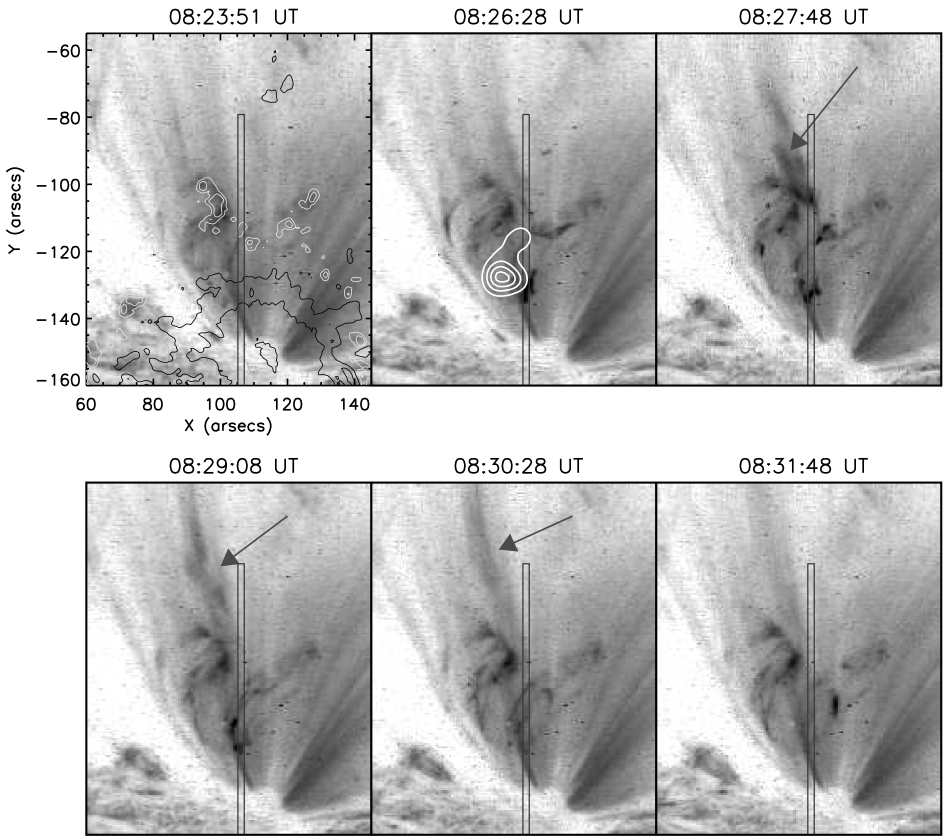

Figure 2: TRACE 17.1 nm image sequence (reversed black/white table) showing the microflare which peaked in X-rays at ∼08:26:30 UT. In the top left panel showing the field of view before the flare, the MDI magnetogram recorded ∼ 45 min earlier is overplotted at isocontours of −1500, −600, −200 (black) and +70, +200 G (white). The RHESSI source associated with the event is overplotted by white contours in the top middle panel (image parameters: energy range 3–8 keV; reconstruction time 08:25:50–08:28:00 UT, contour levels at 20, 50, 90% of the image maximum; Pixon algorithm). The position of the CDS slit is indicated by a black frame in each panel. The appearance and propagation of a jet is indicated by grey arrows.

RHESSI microflares which showed a non-thermal X-ray spectral component. Furthermore, the CDS slit was located at the microflare site. The peak times of the events in the 3–6 keV band were 08:26:20 UT and 08:38:10 UT (cf. Figure 1). Only the first event could be determined to be of GOES class

A9.2/A0.7 with/without background whereas the other microflare was too weak to be observed by GOES.

The TRACE 17.1 nm data for the first event at 08:26 UT reveal a very complex flare sequence (see Figure 2). In the course of the event, several impulsive brightenings situated in magnetic flux of opposite polarity appear. Two of the microflare brightenings ($X_1 \sim 106''$, $Y_1 \sim -130''$; $X_2 \sim 106''$, $Y_2 \sim -110''$) lie directly at the location of the CDS slit.

Although we do not have TRACE imaging information for the second event, we can speculate that the signatures are similar to the other one, as it shows homologous, chromospheric brightenings in the DOT Hα and Ca II channels (not shown here, see Bein *et al.*, 2009).

4. Plasma Flows Observed by CDS

The CDS instrument observed 2 brightenings for each microflare, in both events situated at roughly the same location on the slit ($-110'' < Y_1 < -100''$; $-135'' < Y_2 < -125''$). Each brightening was covering several CDS pixels (pixel size $2'' \times 1.6''$). In the following, we will refer to them as to the 'northern brightening' and 'southern' or 'penumbral' brightening (as it is situated in the penumbra). For the first event, the two foot points lie directly on the slit (see Figure 2). For the second event, the evolution of the CDS intensities compared with the RHESSI X-ray light curve suggests that CDS observed only the decline phase of the event (see Figure 4).

In Figures 3 and 4, we show for each microflare the time evolution of CDS intensities and velocities in selected pixels within the northern and southern CDS brightening (He I and O V). For the first microflare, the He I, O V and Ne VI lines are redshifted indicating plasma flows of ~20–40 km s^{-1} for both brightenings (Figure 3).

For the second event, chromospheric upflows both in He I (10 km s^{-1}), in O V (40 km s^{-1}) as well as in the hotter Ne VI line (40 km s^{-1}) are observed in the penumbral brightening. In the northern brightening, no line shows a clear velocity signal during the flare (see Figure 4).

5. Non-thermal Electrons

The amount of non-thermal energy flux density deposited in the chromosphere determines whether chromospheric evaporation is 'explosive' or

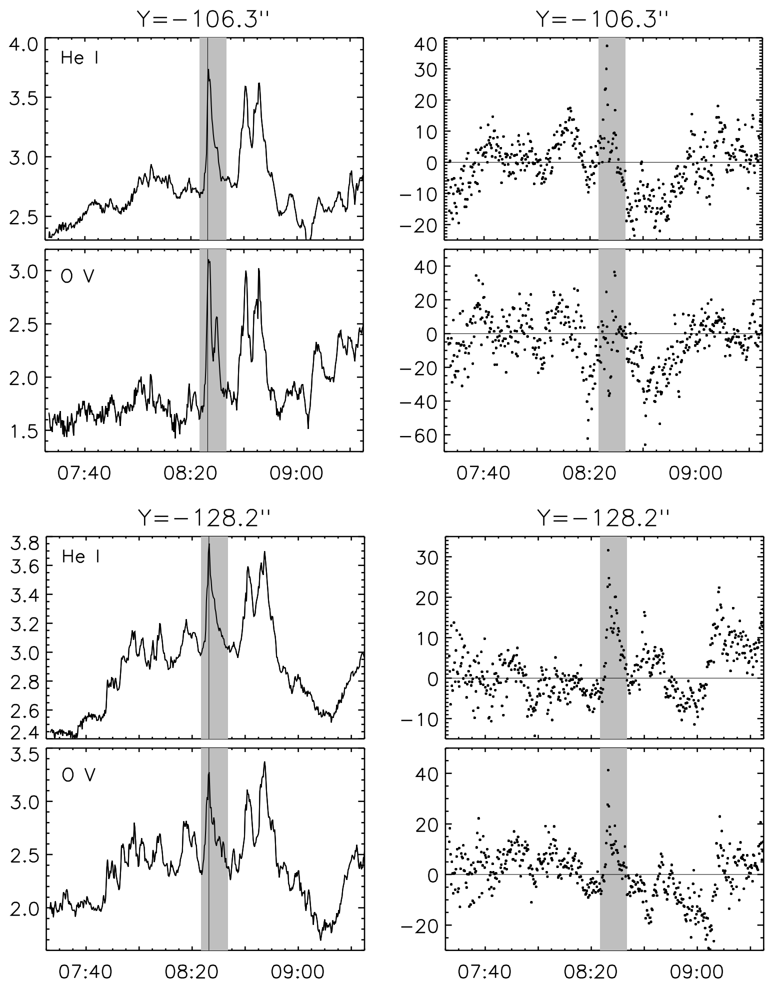

Figure 3: Time development of intensities (left) and Doppler velocities (right) in the CDS He I ($T \sim 3.9 \times 10^4$ K) and O V line ($T \sim 2.6 \times 10^5$ K) observed in selected pixels at the northern ($Y = -106''$) and southern flare brightening ($Y = -128''$) of the 08:26 UT microflare. The grey highlighting marks the period the flare brightenings are located inside the CDS slit. The intensities (solid lines) have units of ergs cm^{-2} s^{-1} sterad^{-1} Å^{-1} and are plotted in logarithmic scale. Velocities are given in units of km s^{-1}. The maximum time in RHESSI X-rays is indicated in the intensity curves by a black line.

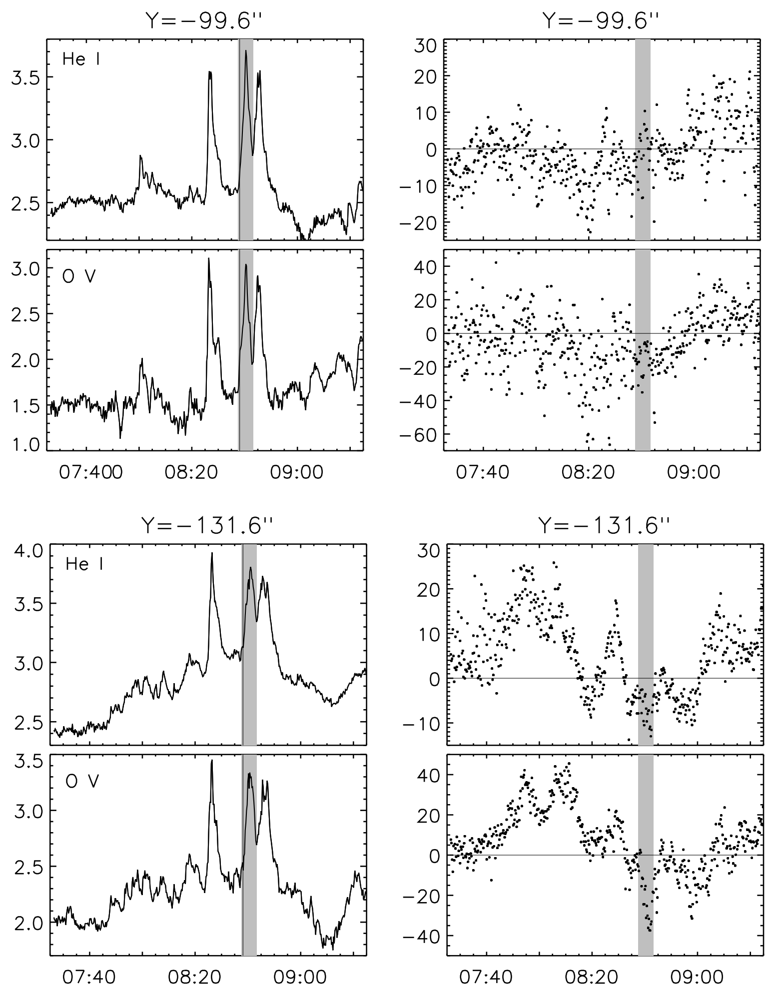

Figure 4: Same as Figure 3 for the microflare which peaked at ∼08:38 UT.

'gentle'. A difference in the characteristics of evaporation might explain why the chromospheric He I line is redshifted for the first and blueshifted for the second microflare. As stated by Fisher *et al.* (1985a), the threshold electron flux density which marks the boundary between explosive and gentle evaporation is $F_{\mathrm{th}} \approx 3 \times 10^{10}$ erg cm^{-2} s^{-1}. With spectral fits of the RHESSI X-ray peak spectrum and imaging of the chromospheric flare brightenings, we are able to determine the electron beam flux density at

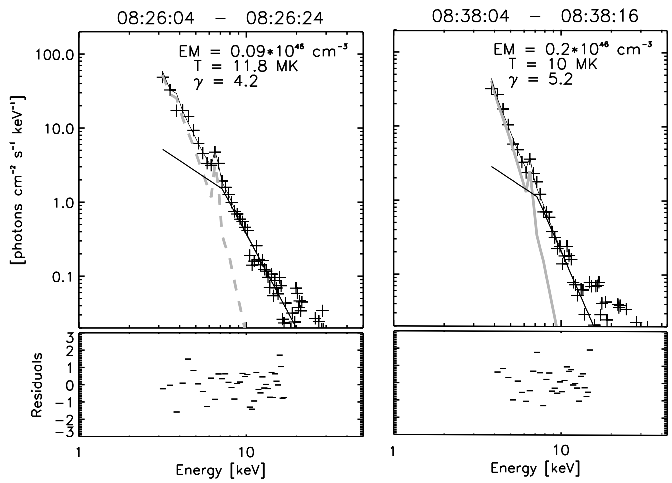

Figure 5: RHESSI photon spectra at an energy resolution of 1/3 keV (crosses) reconstructed at the X-ray peak of the two analysed events. The spectra were fitted with a thermal bremsstrahlung component at low energies (dashed grey line) plus a non-thermal power-law at energies $\gtrsim$9 keV (bold solid line). The sum of both components is plotted as a thin solid line. The normalized residuals are also given for each spectrum shown. The emission measure EM, temperature T and photon spectral index γ are indicated for each event.

the flare peak. Spectral fits showed a power-law component due to non-thermal bremsstrahlung of beamed electrons scattered off ions with rather high photon spectral indices of $\gamma \approx 4.2$ and $\gamma \approx 5.2$ in the 08:26 UT and 08:38 UT event, respectively (Figure 5). Following Stoiser *et al.* (2007), we assume that all electrons with energies $\gtrsim$ 10 keV reach the chromosphere. This is certainly a rather generous estimate. The power of the beam above 10 keV for the two events was determined to $P_{10,1} \approx 1.4 \times 10^{26}$ erg s^{-1} and $P_{10,2} \approx 1.1 \times 10^{26}$ erg s^{-1}. The impact area of the beam was estimated from DOT Hα images (see Bein *et al.* 2009). For the first event, the total area of Hα brightenings[1] was estimated to $5 \times 10^{15} \lesssim A_{\mathrm{f},1} \lesssim 4 \times 10^{16}$ cm^2 and for the second to $4 \times 10^{15} \lesssim A_{\mathrm{f},2} \lesssim 2 \times 10^{16}$ cm^2. The energy flux density $F_1 = P_{10,1}/A_{\mathrm{f},1}$ for the 08:26 UT event thus ranges in between $0.4 \times 10^{10} \lesssim F_1 \lesssim 2.8 \times 10^{10}$ erg cm^{-2} s^{-1}. For the 08:38 UT event, we get $0.6 \times 10^{10} \lesssim F_2 \lesssim 2.8 \times 10^{10}$ erg cm^{-2} s^{-1}. So if all upper limits for

[1]The lower and upper limits of A_f were derived from difference images and the plain Hα maps at the flare peak, respectively.

A_f and P_{10} apply, we find high flux densities close to F_th dividing the explosive and gentle evaporation regime. However, our estimates do not help to explain the different flow directions of the two microflares observed in chromospheric CDS lines.

6. Discussion and Conclusions

Micro-and nanoflare coronal heating models require a multitude of small-scale reconnection events. Therefore it is important to evaluate whether in microflares occur processes which are suggested for regular flares powered by magnetic reconnection, i.e. electron beam driven chromospheric evaporation. The observations presented here are further encouragement for the assumption that the driving mechanism and the flare sequence suggested in the standard eruptive flare model apply as well to microflares. As regarding the chromospheric and transition regional flow pattern associated with the events studied here, the interpretation in the frame of chromospheric evaporation theory and hydrodynamic simulations is difficult. CDS observations of the two microflares indeed indicate the existence of flows in the chromosphere and transition region due to energy input by accelerated electrons. The estimate of the electron energy flux density deposited in the chromosphere is very similar for both events and on the same order of magnitude but nevertheless beneath the threshold value needed for explosive evaporation. However, the microflares show a different flow behaviour in CDS chromospheric and transition region lines, i.e. downflows for the first and upflows for the second event.

Acknowledgements

This work was supported by the exchange program SK-AT-0004-08 of the Fond zur Förderung der wissenschaftlichen Forschung FWF (Austria) and the Slovak Research and Development Agency APVV (Slovakia) as well as by another project of the later agency (APVV-0066-06).

References

Aschwanden, M. J.: 2004, *Physics of the Solar Corona*, Springer, chapter 9, p. 382.

Bein, B., Veronig, A., Rybák, J., *et al.*: 2009, in V. Ruždjak, A. Hanslmeier, and D. Ruždjak (eds), *Cent. Eur. Astrophys. Bull.*, thiss issue.

Brosius, J. W.: 2003, *Astrophys. J.* **586**, 1417.

Brosius, J. W. and Phillips, K. J. H.: 2004, *Astrophys. J.* **613**, 580.

Doschek, G. A., Feldman, U., Kreplin, R. W., and Cohen, L.: 1980, *Astrophys. J.* **239**, 725.

Falchi, A., Teriaca, L., and Maltagliati, L.: 2006, *Solar Phys.* **239**, 193.

Fisher, G. H.: 1989, *Astrophys. J.* **346**, 1019.

Fisher, G. H., Canfield, R. C., and McClymont, A. N.: 1985a, *Astrophys. J.* **289**, 414.

Fisher, G. H., Canfield, R. C., and McClymont, A. N.: 1985b, *Astrophys. J.* **289**, 425.

Fisher, G. H., Canfield, R. C., and McClymont, A. N.: 1985c, *Astrophys. J.* **289**, 434.

Hannah, I. G., Christe, S., Krucker, S., Hurford, G. J., Hudson, H. S., and Lin, R. P.: 2008, *Astrophys. J.* **677**, 704.

Mariska, J. T., Doschek, G. A., and Bentley, R. D.: 1993, *Astrophys. J.* **419**, 418.

Milligan, R. O.: 2008, *Astrophys. J., Lett.* **680**, L157.

Milligan, R. O., Gallagher, P. T., Mathioudakis, M., Bloomfield, D. S., Keenan, F. P., and Schwartz, R. A.: 2006, *Astrophys. J., Lett.* **638**, L117.

Neupert, W. M.: 1968, *Astrophys. J., Lett.* **153**, L59.

Stoiser, S., Veronig, A. M., Aurass, H., and Hanslmeier, A.: 2007, *Solar Phys.* **246**, 339.

Teriaca, L., Falchi, A., Falciani, R., Cauzzi, G., and Maltagliati, L.: 2006, *Astron. Astrophys.* **455**, 1123.